

Focusing light within turbid media with weakly discriminating filters

W. James Tom* and Andrew K. Dunn

The University of Texas at Austin, Austin, Texas 78712, USA

*Corresponding author: wjtom@utexas.edu

Received July 11, 2013; revised December 17, 2013; accepted December 17, 2013;
posted December 18, 2013 (Doc. ID 193746); published February 5, 2014

Many materials, including biological tissue, attenuate light mostly by scattering. Because the scattered field is exquisitely sensitive to perturbations, control over the distribution of light after strong scattering is challenging. Though wavefront-shaping techniques enable arbitrary generation of light distributions within strongly scattering or turbid media in principle, the input wavefront necessary for the chosen light distribution is generally unknown. Using two different computational models, we demonstrate a technique called virtual aperture culling of the eigenmodes of a resonator (VACER), which uses weak spatial filtering mechanisms for noninvasive light focusing at arbitrary positions within turbid media. Compatibility with weak spatial filtering mechanisms is critical to innocuously focusing light within turbid media. One model represents an ideal system and could be physically implemented in some scenarios with digital optical phase conjugation, while the other model simulates phase conjugation via gain saturation, and its physical realization would operate fast enough to avoid the effects of speckle decorrelation in biological tissue. Modeling results establish that sound physical principles underlie VACER. © 2014 Optical Society of America

OCIS codes: (170.7050) Turbid media; (290.7050) Turbid media; (190.5040) Phase conjugation; (170.3660) Light propagation in tissues; (140.3325) Laser coupling; (140.3535) Lasers, phase conjugate.
<http://dx.doi.org/10.1364/JOSAB.31.000412>

1. INTRODUCTION

Applications of light in many media, including biological tissue, are limited by scattering. Although scattering is often considered stochastic, scattering is actually deterministic. Scattering is a process involving the coupling of a set of input modes to a set of output modes. For a turbid medium, the relationship between the input and output modes and the internal modes, which are generally accessible only by invasive means, is unknown. Only the external (input and output) modes can be easily controlled or measured. The most significant challenges associated with turbid media originate from this property. Despite the success of wavefront shaping and phase conjugation in mitigating scattering issues [1–8], directing light to a chosen location within turbid media has not been achieved without caveats.

In principle, a technique named time-reversed ultrasonically encoded (TRUE) optical focusing [9] is able to focus light at arbitrary positions within turbid media. An ultrasonic wave is focused on the target within a turbid medium. As long as the scattering of ultrasonic waves is significantly less than light scattering, the ultrasonic focus is largely unperturbed by the turbid medium. When a coherent light source illuminates the turbid medium, some of the light is frequency shifted through interaction with the ultrasonic wave within the turbid medium. The scattered light can be collected to form a hologram for phase conjugation. If the reference wave used for hologram formation is frequency matched to the ultrasound-modulated light rather than the light source, then phase conjugation with the hologram yields a phase conjugate wave consisting primarily of the phase conjugate of the ultrasound-modulated light. Thus, a phase conjugate wave is

generated which is focused on the ultrasonic focus. Though TRUE optical focusing is conceptually complete, some problems exist. First of all, the light focus cannot be smaller than the ultrasonic focus with techniques like TRUE optical focusing. Thus, optical resolutions are out of reach. However, the most significant limitation is that modulation of light with ultrasound in turbid media is very inefficient. In previous experiments, only on the order of 10^{-4} of the transmitted light is frequency shifted by the ultrasound [10]. With little modulated light, it is difficult to form a hologram for phase conjugation, and consequently the quality of the light focus suffers. The light focus becomes larger and less sharp. The same issue with the inefficiency of ultrasonic modulation leads to low signal-to-noise ratio in ultrasound-modulated optical tomography [11,12] and has been a considerable obstacle to the development of ultrasound-modulated optical tomography applications.

Considerable background signal has been observed experimentally in derivative techniques of TRUE optical focusing. Signal-to-background ratios of 5.5 [10] and 1.5–4 [13] have been observed experimentally. Although phase conjugation of only part of the scattered field limits time-reversal reproduction accuracy [14,15], the observed background signal is much higher than would be expected if partial phase conjugation is the limitation in phase conjugation fidelity [16]. In an earlier study with a comparable system, phase conjugating a spatially filtered beam rather than ultrasound-modulated light yielded signal-to-background ratios of about 600 [7]. With the portion of the phase-conjugated field being fixed, iterative application of TRUE optical focusing has been shown to reduce the background signal. After nine iterations,

the background decreased by a factor of 5 relative to the signal [17]. The substantial background light in TRUE optical focusing and similar techniques arises because ultrasound modulation does not discriminate against modes strongly enough to limit the quantity of phase-conjugated modes.

Unfortunately, there do not appear to be any efficient and innocuous methods to filter light based on position within most turbid media. Like ultrasonic modulation of light in turbid media, they all seem inefficient. Thus, there is a choice between positive selection with low background signal but low efficiency and negative selection with high efficiency but high background signal. With either choice, there is little difference between the signal and the background. TRUE optical focusing and its derivatives rely on positive selection methods and suffer from inefficiency. Despite the ultrasonic filtering process having low background signal, the difference in the magnitude of the signal and the background is small. Thus, the optical focus is not very prominent.

First, we will describe virtual aperture culling of the eigenmodes of a resonator (VACER) on a conceptual level and the means by which it enhances weak filters. Then, modeling of an ideal VACER system will reveal the ability of VACER to focus light within turbid media and the similarity of VACER to previous experimental work with iterative application of TRUE optical focusing. Moreover, the relative simplicity of ideal VACER will facilitate intuitive comprehension. Finally, modeling of a VACER system relying on phase conjugation through gain saturation will demonstrate sufficiently fast operation to avoid the deleterious effects of speckle decorrelation at the expense of much more complicated dynamics due to minor deviations from ideal VACER properties.

2. CONCEPT

VACER is an approach to focusing light at arbitrary positions within turbid media [18]. Similar to other techniques involving wavefront shaping or phase conjugation in turbid media, VACER exploits the determinism of scattering. Unlike other methods, a virtual aperture establishes the position of the focus. Moreover, the turbid medium is placed within a phase conjugate resonator, an optical cavity terminated by phase conjugate mirrors on both ends. Rather than merely reflect waves, a phase conjugate mirror phase conjugates incident waves, leading to time reversal in time-reversal symmetric media.

When a pulse of coherent light seeds the resonator through one of the phase conjugate mirrors, as seen in Fig. 1(a), the light is scattered and possibly partially absorbed while traversing the turbid medium. After reaching the second phase conjugate mirror, the scattered light is phase conjugated. As in Fig. 1(b), the light returning to the first phase conjugate mirror approximates a time-reversed replica of the original seed pulse traveling in the opposite direction. After phase conjugation by the first phase conjugate mirror, the light again propagates through the turbid medium, back toward the second phase conjugate mirror. After many cycles between propagating through the turbid medium and phase conjugation by the phase conjugate mirrors, only the light occupying the modes of high transmission will remain, as seen in Fig. 1(c). Nevertheless, eventually all of the light is absorbed or lost by other mechanisms.

Introducing increasing amounts of optical amplification into a phase conjugate resonator increases the lifetime of modes within the phase conjugate resonator until the gain exceeds the loss, at which point stable oscillation or lasing becomes possible. Contrasting with typical lasers, the transverse modes of a phase conjugate resonator with a turbid medium cannot be described by Hermite–Gaussian or Laguerre–Gaussian expansions, and the phase conjugate resonator has no intrinsic longitudinal mode selectivity. Moreover, the mode structure depends on the exact configuration and orientation of the turbid medium. When a sufficiently accurate approximation of time reversal is achieved by the phase conjugate mirrors, light absorption within the stable modes is less than the absorption predicted by diffusion models of light propagation because the stable modes tend to avoid regions of high absorption. Therefore, even with large circulating powers, absorption and thus damage potential is minimal.

Modes within the turbid medium are culled with a virtual aperture. The virtual aperture can be implemented by any mechanism which enables filtration of light based on position. The center of the virtual aperture is the position at which the mechanism attenuates light the least. A virtual aperture could be constructed by introducing magnetic fields to induce the Faraday effect. Because the polarization rotation caused by the Faraday effect is nonreciprocal, no phase conjugate mirror can reverse the polarization rotation. When polarization selectivity exists in either the turbid medium or the phase conjugate resonator, light traveling through regions with a magnetic field are attenuated. Thus, with carefully crafted magnetic field geometry, optical modes can be culled as seen in Fig. 1(d). Compared to other possible discrimination mechanisms, magnetic fields are appealing because static magnetic fields are usually harmless to nonmagnetic media and are influenced insignificantly by many materials, including biological tissue. However, attenuation from magnetic fields would likely be very weak. A virtual aperture formed by ultrasound waves would be ineffective in a medium with substantial mechanical impedance inhomogeneities but would generally discriminate modes more strongly than magnetic fields in any of the many materials of limited mechanical heterogeneity.

The virtual aperture enables localization of diffuse light. Because a minor impediment on each pass becomes a significant disadvantage after many cycles back and forth in the phase conjugate resonator, weak mode discrimination mechanisms suffice for virtual apertures capable of light focusing in turbid media with considerable light concentration. If any modes are permitted to bypass the virtual aperture, then control conferred by the virtual aperture over where the light is focused is lost. Only modes which travel through the center of the virtual aperture should be able to avoid attenuation by the virtual aperture.

3. IDEAL MODEL

Two phase conjugate mirrors separated by a turbid medium are modeled. The ideal assumptions described in this section apply to the phase conjugate mirrors only. We assume that the VACER system proper behaves ideally, but we impose no such limitations on the turbid medium.

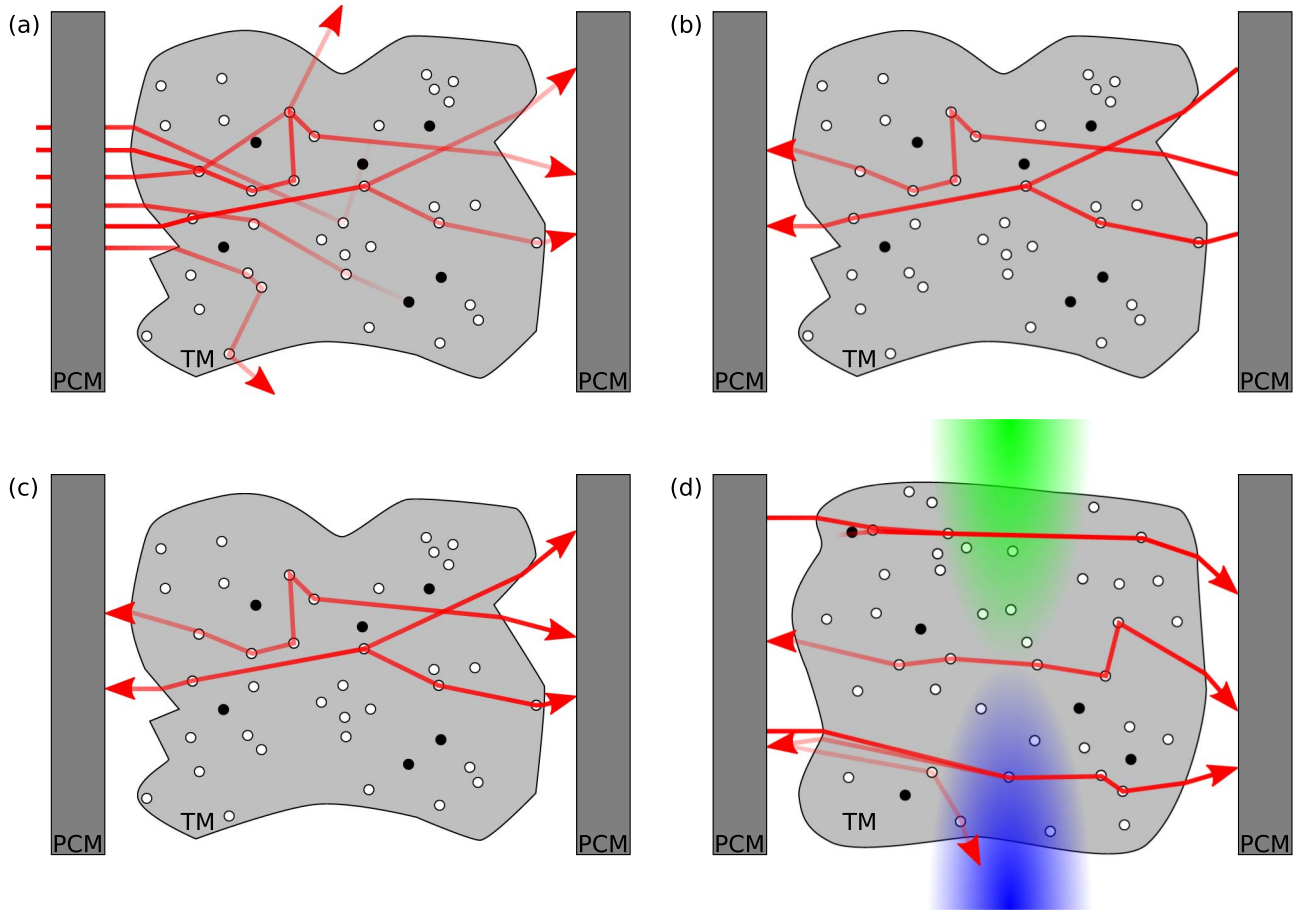


Fig. 1. (a) Pulse of seed light passes through the first phase conjugate mirror, PCM. Though some of the light is attenuated by absorbers (black circles) and scatterers (white circles) in the turbid medium (TM), some of the light reaches the second PCM. (b) The light which reaches the second PCM is phase conjugated and travels back toward the first PCM by traversing its path in the opposite direction. (c) The light which continually cycles from one PCM through the TM to the other PCM constitutes the stable modes of the phase conjugate resonator. An actual phase conjugate resonator may support countless optical modes. Moreover, cavity gain ensures that the modes contain many photons. The total circulating power of the phase conjugate resonator can be very high without causing damage because photons are concentrated in modes with low absorption. (d) Neither PCM is able to invert nonreciprocal effects such as the Faraday effect, which is the nonreciprocal polarization rotation of light in a medium with an axial magnetic field. Consequently, processes such as scattering that generally exhibit polarization dependence are altered with each pass through the TM. Modes can be perturbed such that light is lost from the phase conjugate resonator by absorption (upper mode) or scattering (lower mode). The modes which avoid the axial magnetic fields tend to be attenuated the least and have the highest probability of becoming stable modes (middle mode). The upper magnetic field (green) directed toward the right decreases with distance (diminishing green intensity) from an unseen magnet from above, while the lower magnetic field (blue) directed toward the left decreases with distance (diminishing blue intensity) from an unseen magnet from below.

A. Ideal Assumptions

In order to simplify analysis, we introduce two idealizations. First, we assume that phase conjugation is free of distortion. Linear phase conjugation represented by function f satisfies

$$f\left(\sum_n E_n\right) = \sum_n f(E_n) \quad (1)$$

and

$$f(\eta E_n) = \eta f(E_n), \quad (2)$$

while distortion-free phase conjugation represented by function g satisfies only

$$g\left(\sum_n E_n\right) = \gamma \sum_n f(E_n) \quad (3)$$

for each wave E_n . Observe that this assumption does not imply complete linearity. In general,

$$g(\eta E_n) \neq \eta g(E_n). \quad (4)$$

Second, we assume that mode competition is such that each mode, when sufficiently powerful, can reduce the gain of every other mode to below the threshold value.

B. Computational Efficiency Assumptions

For computational efficiency, we employ two simplifications. First, we assume that the fields change slowly enough that discrete updates to the phase conjugate waves are a satisfactory approximation of continuous updates. Second, we assume that the time required for the phase conjugate mirrors to adapt to a new wavefront is much longer than the time required for light to propagate from one phase conjugate mirror, through the turbid medium, to the other phase conjugate mirror. Hence, between updates to the phase

conjugate waves, the fields within the system approach steady state.

C. Energy Conservation

To keep energy finite, the phase conjugate wave is scaled so that the amplitude of the highest amplitude component is fixed. Consequently, the second ideal assumption regarding mode competition is achieved while maintaining compliance with the condition that phase conjugation be distortion-free, represented by Eq. (3). The highest amplitude component may change with each iteration.

D. Physical Interpretation

With a few notable differences, the two ideal assumptions and the two computational efficiency assumptions result in a model which represents a system with remarkable similarity to iterative TRUE application, which has been experimentally demonstrated with digital optical phase conjugation [17]. In digital optical phase conjugation, the wavefront is determined by digital holography, and then the phase conjugate wave is produced with a spatial light modulator. There are three major differences between the physical interpretation of the model and the experimental demonstration of iterative TRUE application. First, phase conjugation which accounts for amplitude and phase, rather than phase only, is employed. Second, we assume that noise such as shot noise is negligible in the determination of the phase conjugate wavefront. Third, we assume that phase conjugate reproduction errors are negligible. In particular, design limitations and manufacturing defects of the spatial light modulator used for phase conjugate generation yield no discernible phase conjugate imperfections. Some robustness of phase conjugation to phase errors has been experimentally observed [7].

E. Turbid Media Model

Scattering may be represented by complex transfer matrices which describe the coupling of input modes to output modes. Mathematically describing turbid media with transfer matrices has been experimentally validated in the continuous wave case [19,20]. The turbid medium models used here are layered structures. Scattering occurs at the interfaces between layers. Consequently, wave propagation between layers is characterized by complex scattering matrices. Between layers m and $m + 1$,

$$\begin{bmatrix} \mathbf{B}_{m,1} \\ \mathbf{F}_{m+1,0} \end{bmatrix} = \mathbf{M}_m \begin{bmatrix} \mathbf{F}_{m,1} \\ \mathbf{B}_{m+1,0} \end{bmatrix}, \quad (5)$$

where $\mathbf{F}_{m,1}$ and $\mathbf{F}_{m+1,0}$ are vectors of the complex amplitudes of the modes propagating forward at the distal interface of layer m and the proximal interface of layer $m + 1$, respectively; $\mathbf{B}_{m,1}$ and $\mathbf{B}_{m+1,0}$ are vectors of the complex amplitudes of the modes propagating backward at the distal interface of layer m and the proximal interface of layer $m + 1$, respectively; and \mathbf{M}_m is the complex scattering matrix coupling the modes of layer m and layer $m + 1$. Transmission through each layer is lossless.

With a few noted exceptions, the scattering matrices used here do not have backscatter and become unitary when multiplied by the appropriate real scalar greater than 1. Each unitary matrix is randomly selected from the circular unitary

ensemble [21]. A notable exception exists in the plane of every virtual aperture, where the transmission eigenvalues of the selected and culled modes usually differ.

Only a fraction of the number of modes in actual turbid media are modeled due to limited computational resources. Computational demands of the model presented in the following section are particularly limiting in the number of layers and the modes per layer. Nevertheless, the systems are turbid in the sense that the fields of the internal modes are unknown even when the fields of the input and output modes are known and controllable. Most of the simulations model turbid media with 10 layers and 8 modes per layer. Hence, each system has 16 external modes and 64 internal modes.

F. Simulation Initiation

The seed light initiates all input modes with waves of the same amplitude and phase, which simulates the incidence of a beam or other wave with a relatively flat wavefront, yet the initial energy in the selected and culled modes depends on the scattering of the turbid medium.

G. Results

In an ideal VACER system, the power in the selected mode increases while the power in the culled modes decreases indefinitely. In Fig. 2, the culled modes decay exponentially once the power in the selected mode nears its asymptotic value. Moreover, by comparing Fig. 2(a) to Figs. 2(b) and 2(c), it is evident that the decay constant is proportional to the transmittance of the culled modes relative to the selected mode transmittance. Scattering randomizes the initial power distribution among modes, as observed when comparing Figs. 2(b) and 2(c). Because the transmittance of the culled modes is equal, the power distribution among culled modes is persistent. A cycle consists of two updates to the phase conjugate waves. In a cycle, most of the light travels forward first, and then most of light travels backward. Power is normalized such that the power of the mode of the phase conjugate wave with the most power is 1, yet the normalized power in the selected mode may exceed 1.

When the loss outside of the virtual aperture is heterogeneous, part of the scattered field is lost. Hence, phase conjugation is necessarily incomplete. If phase conjugation is partial, modes have an unavoidable coupling. In Fig. 3, power from the selected mode leaks into the culled modes since the phase conjugation is incomplete. Consequently, the power in the culled modes becomes stable. Like partial phase conjugation, backscattering within the turbid medium leads to inescapable mode coupling. Figure 4 shows that the power in the culled modes does not decay indefinitely with backscatter. In fact, the power in one of the culled modes appears to rise monotonically to an asymptote as the power in the selected mode increases toward its stable value. An alternative explanation for the performance degradation is that backscatter results in multiple traversals of the virtual aperture, and passage of the selected mode exclusively through the center of the virtual aperture becomes improbable in the presence of scattering and other mechanisms of divergence. Reversing the source and target by hypothetically placing a continuous-wave light source at the center of the virtual aperture enables determination of the maximum power concentration allowed by a particular medium by any method. By applying

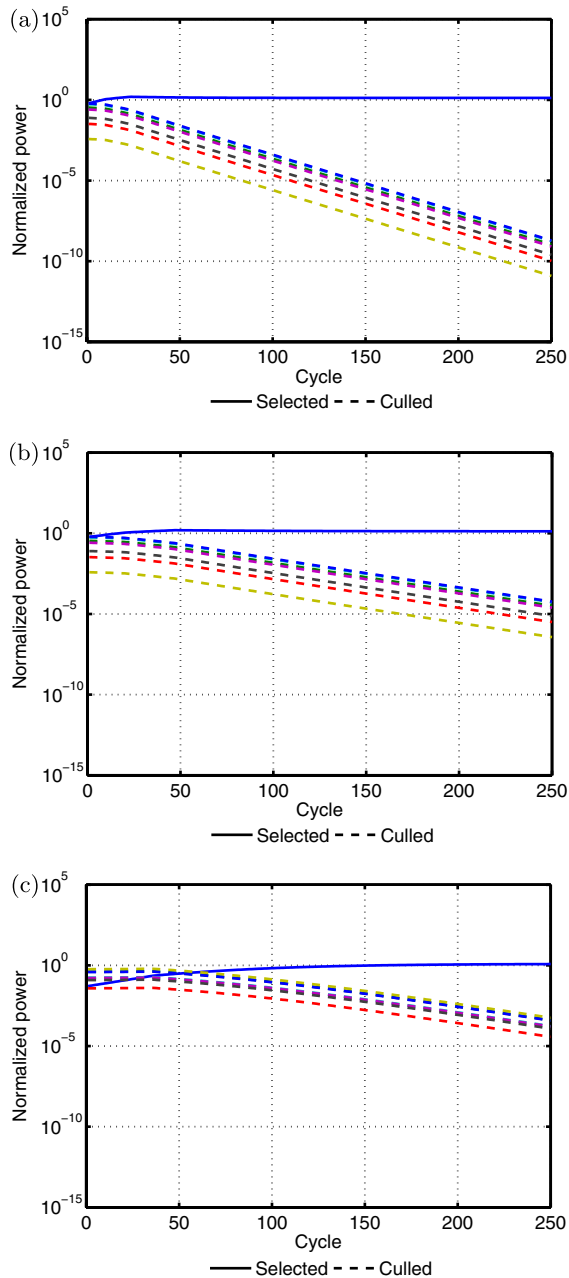


Fig. 2. In these three representative time series of the idealized VACER model, virtually all of the circulating power is in the selected mode (solid line) by the end of the simulations because the power in the seven culled modes (dashed lines) perpetually decays. In (a), the transmittance of the culled modes is 4% less than the transmittance of the selected mode, while in (b) and (c), the transmittance of the culled modes is 2% less. Though (a) and (b) result from simulations with the same randomly generated turbid medium, (c) originates from a distinct turbid medium.

such a thorough experiment, we conclude that some diminution of power concentration is unavoidable for all methods in media with backscatter and divergence due to the diffusion of power on subsequent backscatter-induced passes. Though performance is variable, intrinsic mode coupling limits the power concentration achievable by any phase conjugation or wavefront-shaping scheme, including VACER.

Without partial phase conjugation and backscatter, Fig. 5 indicates that, because the power in each mode is scaled

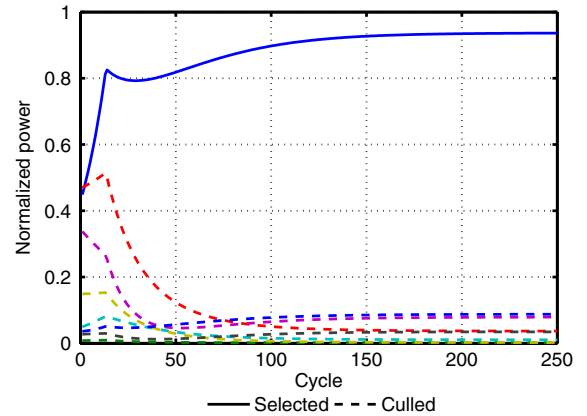


Fig. 3. In this time series with partial phase conjugation, the selected mode (solid line) eventually has more power than the seven culled modes (dashed lines), but the culled modes do not continually diminish. Generally, incomplete phase conjugation couples the selected mode to the culled modes, which even an idealized VACER system cannot prevent. The transmittance of the culled modes is 2% less than the transmittance of the selected mode.

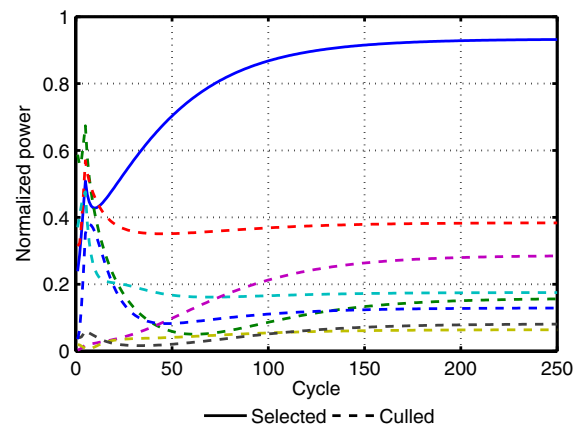


Fig. 4. In this time series with backscatter, the selected mode (solid line) eventually has more power than the seven culled modes (dashed lines), but the culled modes do not continually diminish. Generally, backscatter couples the selected mode to the culled modes, which even an idealized VACER system cannot prevent. In this example, the turbid medium backscatters about 7.5% of the incident light. The transmittance of the culled modes is 2% less than the transmittance of the selected mode.

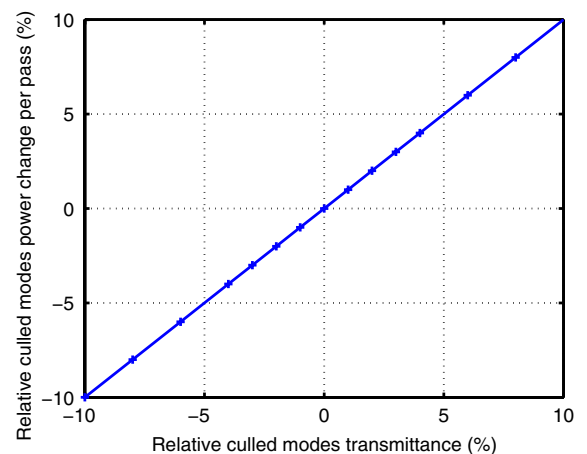


Fig. 5. In the idealized VACER model, the relative change per pass in the power of the culled modes is merely the relative transmittance of the culled modes.

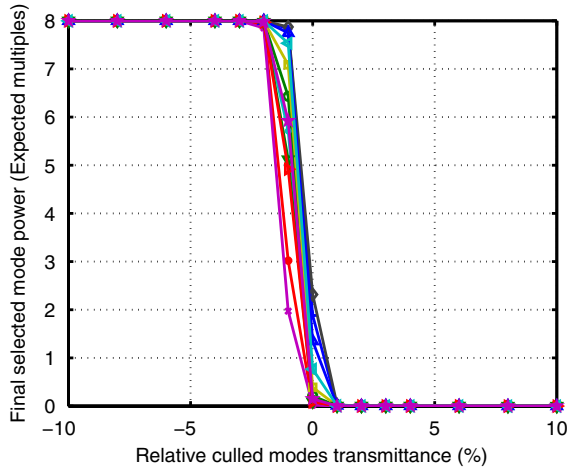


Fig. 6. Final power in the selected mode depends on the transmittance of the culled modes. While nearly all of the power is in the selected mode, given time, when the culled mode transmittance is less than the selected mode transmittance, the selected mode has negligible power when culled mode transmittance is greater than selected mode transmittance. Each plotted curve is from a different randomly generated turbid medium.

by the respective transmittance on each pass, the power in the culled modes relative to the power in the selected mode changes by the transmittance of the culled modes relative to the transmittance of the selected mode with each pass. For example, when the transmittance of the culled modes is 10% less than the selected mode transmittance, the power in the culled modes becomes 10% less relative to the selected mode power as compared to the previous pass, or 19% less as compared to the previous cycle.

In an ideal VACER system, most of the power ends up in the selected mode, given enough time, if the selected mode transmittance is greater than the transmittance of the culled modes and there is no inherent mode coupling. In Fig. 6, the difference in power concentration in the selected mode in different turbid media is negligible, after 250 cycles, when the transmittance discrepancy between the selected and culled modes is greater than or equal to 2%. With 1 selected mode and 7 culled modes, the selected mode is expected to have 12.5% of the total power, but VACER can achieve significantly more. As the power in the selected mode approaches the total power, the selected mode power nears 8 times the expected power. Thus, in an ideal VACER system, after an adequate wait, there is a negligible difference in power concentration in the absence of intrinsic mode coupling.

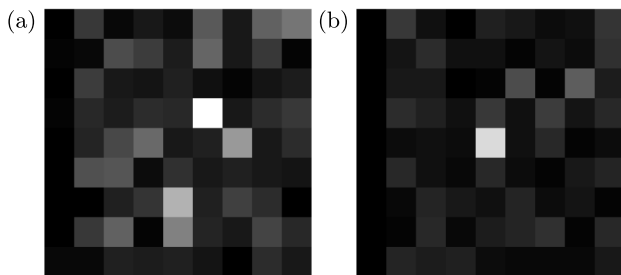


Fig. 7. (a) After one cycle, very little power is in the selected mode at the center of the image. (b) After 250 cycles, the selected mode has the most power.

Since concentrating power within selected modes amounts to light focusing, VACER can focus light within turbid media. The images in Fig. 7 represent the power distribution in the plane of the virtual aperture for a simulation with 21 layers and 81 modes per layer, which is increased from the 10 layers and 8 modes per layer used in the simulations underlying the five previous figures. Moreover, backscatter and partial phase conjugation have been modeled. After 250 cycles, the selected mode has the most power despite very little power being in the selected mode after a single cycle.

4. FAST MODEL

Now we model a VACER system that deviates from ideal behavior but has a very short response time. Hence, we refer to this model as the fast model. The computational demands of the fast model are significantly higher than the ideal model. Commonly used approaches such as finite-difference time-domain methods are unsuitable because the computational demands are too great. In order to represent feasible experimental systems, the length of the modeled systems needs to be on the order of 100,000 wavelengths, and simulations must last on the order of 1,000,000,000 wave periods.

Each end of the modeled resonator is a phase conjugate mirror implemented by wave mixing in a gain medium. The turbid medium lies between the phase conjugate mirrors. Rather than explicitly modeling phase conjugation, wave mixing leads to phase conjugation. The axial small signal gain of each gain medium is 100, but the phase conjugate reflectivity is much less. The wave mixing model is adapted from coupled mode theory methods widely used in the analysis and design of diffraction gratings. Each gain medium has two high-powered counterpropagating reference beams. The irradiance of each reference beam in the gain media is $0.01I_s$ where I_s is the saturation irradiance of the gain medium. All four reference beams are mutually coherent. Time is measured in multiples of the lifetime of the atomic population of the upper energy level of the lasing transition in the gain media in the absence of electromagnetic radiation. Light propagation between gain media requires half of a lifetime, while propagation through each gain medium requires about 8×10^{-3} lifetimes.

A. Gain Media Model

The complex electric field E_p of plane wave p is

$$E_p = A_p \exp(-i\mathbf{k}_p \cdot \mathbf{r}) \exp(i\omega t), \quad (6)$$

where A_p is the complex envelope of a modulated monochromatic plane wave with wave vector \mathbf{k}_p and angular frequency ω . Both inside and outside of the gain media, light is propagated using the slowly varying envelope approximation.

$$-2i|\mathbf{k}_p| \cos \theta_p \frac{\partial A_p}{\partial \xi} - \frac{2i|\mathbf{k}_p|}{c} \frac{\partial A_p}{\partial t} = -\mu\omega^2 F_p, \quad (7)$$

where ξ is the position along the axis of the gain medium. The angle between the wave vector \mathbf{k}_p and the axis of the gain medium is θ_p . The speed of light c in the host medium is

$$c = \frac{1}{\sqrt{\mu\epsilon}}, \quad (8)$$

where μ is the permeability of the host medium and ϵ is the permittivity of the host medium. The complex polarization density P of isotropic media may be expressed as

$$P = \sum_p F_p \exp(-i\mathbf{k}_p \cdot \mathbf{r}) \exp(i\omega t) = \epsilon\chi \sum_p E_p, \quad (9)$$

where the electric susceptibility χ is linearly proportional to the population density difference N . F_p is always zero outside of gain media. Waves propagating in opposite directions are handled as distinct modes. Dispersion is assumed to be negligible. The population density difference N is described by a system of semiclassical rate equations derived from

$$\begin{aligned} \frac{\partial N}{\partial t} = & R - \frac{1}{\tau} \sum_n N_n \exp(-i\mathbf{K}_n \cdot \mathbf{r}) \\ & - \frac{c}{2\tau I_s} \sum_n N_n \exp(-i\mathbf{K}_n \cdot \mathbf{r}) \text{Re} \left[\epsilon \sum_p \sum_q E_p E_q^* \right], \end{aligned} \quad (10)$$

where R is the pumping rate, τ is the lifetime of the atomic population of the upper energy level of the lasing transition in the gain media, and

$$I_s = \frac{\hbar\omega}{\sigma\tau}. \quad (11)$$

Here, \hbar is the reduced Planck constant, and σ is the emission cross section of the atomic population of the upper energy level of the lasing transition in the gain media. Though the complex electric field E_p is a function of space \mathbf{r} and time t , the complex envelope A_p is a function of only the axial position ξ and time t . Likewise, the population density difference N is a function of space \mathbf{r} and time t , but each N_n is function of only the axial position ξ and time t . Using the method of lines and approximating the spatial derivatives by high-order finite differences, the partial differential equations representing the entire system are converted to a system of ordinary differential equations which are solved with a second-order implicit ordinary differential equation solver [22]. Though usage of an implicit ordinary differential equation solver limits scalability to large problems, numerical stability is maintained with large time steps.

Spontaneous emission is not modeled because it is likely to be inconsequential, unlike in most lasers in which lasing arises from spontaneous emission. In order for the spontaneous emission to be insignificant, stimulated emission must be much greater than the spontaneous emission in each mode. The scenario in which satisfying the assumption that spontaneous emission is negligible is most difficult when the spontaneous emission is greatest. This occurs when all of the spontaneous emission is coupled into the turbid medium. In this scenario, the amount of the spontaneous emission in the turbid medium is the pump power scaled by the quantum efficiency less the amount of stimulated emission. Hence, the stimulated emission must exceed half of the pump power scaled by the quantum efficiency for the stimulated emission to be greater than the spontaneous emission. Of course, in virtually all scenarios, only a small fraction of spontaneous emission will couple into the turbid medium; the spontaneous emission of the gain media radiates in every direction while the stimulated emission is only in the modes of

interest. Consequently, the spontaneous emission into each mode of interest will tend to be negligible, and the spontaneous emission coherent with the reference waves will be even less because the spontaneous emission will be distributed over the transition linewidth.

B. Mode Overlap

For computational efficiency, the external modes are modeled as plane waves. Considering that, for high gain in any experimental implementation, the external modes would be focused into the gain media, the waves would be approximately plane waves near the focus. The approximation of the external modes as plane waves within the gain media implies that the irradiance of each mode is transversely uniform within the gain media. Consequently, the external mode overlap is 100%. With uniform irradiance, mode overlap is merely the geometric intersection of the mode volumes in a gain medium. In this work, external mode overlap is expressed as a fraction. The external mode overlap of external mode A with external mode B is the volume of the intersection between the modes in a gain medium divided by the total volume of external mode A in the gain medium. Because all external modes have the same mode volume in the gain media in the model used here, the external mode overlap of external mode B with external mode A is equal to the external mode overlap of external mode A with external mode B. Mode overlap is a critical parameter in determining the nature of the competition between two modes.

Because 100% mode overlap is only possible in special circumstances such as counterpropagating beams, partial mode overlap is modeled. Portions of the external modes are picked off for external mode overlap other than 100%. The picked off light from each mode is directed to a separate gain medium, while the remaining light is sent to a shared gain medium. Thus, there is mode overlap in the shared gain medium but not in the private gain media. The phase conjugate waves from each gain medium recombine to form the phase conjugates of the external modes with variable fidelity. Modeling variable amounts of mode overlap necessitates modeling phase conjugation imperfection of the external modes.

Less faithful time-reversed reconstructions of the external modes couple less efficiently to the modes of the turbid medium. Imagine phase conjugation of the light from a single-mode optical fiber. If phase conjugation yields a time-reversed replica of the wave emitted from the optical fiber, the phase conjugate wave will couple to the optical fiber with high efficiency. If phase conjugation produces a distorted reproduction of the wave emitted from the optical fiber, much of the phase conjugate wave will not couple into the optical fiber. Alternatively, consider transmission through a small aperture. If the phase conjugate mirror phase conjugates only a portion of the wave transmitted through the aperture in the forward direction, then the time-reversed wave will be larger than the aperture at the aperture plane and hence be partially blocked. Though modeling coupling efficiency of the external modes into the turbid medium as optical fiber coupling or transmission through an aperture would lead to a simple experimental version of the computational model, the computational costs would be high at each time step. As a compromise between physical realizability and computational efficiency, the computational model abstracts the coupling

efficiency as a process of beam recombining with beam splitters.

The amplitude A_u of the u th output mode of the turbid medium is separated into two waves by an ideal beam splitter. S_u is the amplitude of the wave directed toward the shared gain pool, while P_u is the amplitude of the wave directed toward the private gain pool

$$\begin{bmatrix} S_u \\ P_u \end{bmatrix} = \frac{1}{\sqrt{2}} \begin{bmatrix} 1 & i \\ i & 1 \end{bmatrix} \begin{bmatrix} A_u \\ 0 \end{bmatrix}. \quad (12)$$

For the v th external mode propagating into the turbid medium, S_v and P_v are the amplitudes of the waves emerging from the shared and private gain pools, respectively. They propagate into separate ports of an ideal beam splitter

$$\begin{bmatrix} A_v \\ x \end{bmatrix} = \frac{1}{\sqrt{2}} \begin{bmatrix} 1 & i \\ i & 1 \end{bmatrix} \begin{bmatrix} S_v \\ P_v \end{bmatrix}, \quad (13)$$

where A_v is the amplitude of the v th input mode of the turbid medium. The power represented by x is wasted. As S_v and P_v approach scaled phase conjugates of S_u and P_u , x approaches 0, and hence efficiency of coupling to the turbid medium approaches 100%.

In this work, each external mode has a private gain pool, and there is a gain pool shared by all eight external modes in each phase conjugate mirror. Thus, each external mode has an overlap of 50% with the seven other external modes in each phase conjugate mirror. Many other external mode overlap scenarios are conceivable. There could be four nonoverlapping pairs of overlapping modes. Another possibility is having seven partially overlapped modes while the eighth does not overlap any of the other modes.

C. Nonideal Characteristics

Because the phase conjugate mirror model using gain media strives for realism, neither of the two ideal assumptions are satisfied in the fast model. While the first assumption is approximated by the fast model, waves with slightly different incidence angles are amplified by slightly different amounts because having different incidence angles results in slightly different path lengths in the gain media. The second assumption would be true in the fast model if the mode overlap between each mode and every other mode is 100%, which, as mentioned previously, is rarely possible.

D. Turbid Media Model

Unlike the idealized model from the previous section, propagation delay must be simulated in the fast model. Hence, the components of $\mathbf{F}_{m,1}$ at the distal interface of layer m result from wave propagation of the components of $\mathbf{F}_{m,0}$ at the proximal interface of layer m using Eq. (7). Conversely, the components of $\mathbf{B}_{m,0}$ at the proximal interface of layer m arise from backward propagation of the components of $\mathbf{B}_{m,1}$ at the distal interface of layer m .

E. Simulation Initiation

To initiate a simulation trial, a seed pulse is introduced through one of the gain media. The seed pulse is coherent with all four of the reference beams. The duration of the seed pulse is twice the time required for light to travel from one phase

conjugate mirror to the other. The seed pulse ensures oscillation from one phase conjugate mirror through the virtual aperture to the other phase conjugate mirror. If some oscillating modes avoid the virtual aperture, then control exerted by the virtual aperture over where light is focused within the turbid medium is disrupted. The modes with the lowest losses must travel through the center of the virtual aperture for VACER to operate as intended.

F. Results

Figure 8 demonstrates the ability of VACER implemented with a fast phase conjugation method to concentrate light within a selected mode. Dimensionless power is the irradiance divided by I_s integrated over a unit area. If the atomic lifetime τ is 10 ns, then each simulation shown in Fig. 8 spans only 10 μ s. The speed and potential for dynamic wavefront adaptation with VACER are important for mitigating speckle decorrelation [23].

Though the power in all eight modes initially rises, the power in the single selected mode grows the most, and eventually the power of the selected mode is high enough to saturate the gain sufficiently to nearly inhibit oscillation of the seven culled modes. Nevertheless, the power in each culled mode reaches a nonzero stable value because neither of the two idealizations from the ideal model are satisfied. The phase conjugation is imperfect, and mode competition does not permit complete suppression of one mode by another since the mode overlap is not 100%.

Nonetheless, mode competition is more practical for maximizing the selected modes while minimizing the culled modes than reducing the gain until the culled modes are below threshold. Adjusting the gain to drop the culled modes below threshold is very difficult when the difference in transmittance between the selected and culled modes is small, as would generally be the case. Moreover, when gain is decreased until the culled modes cease oscillation and the transmittance difference between the selected and culled modes is slight, the selected modes have little power.

Not only does the fast model exhibit suboptimal performance, but its behavior is also much more complicated and variable than the consistent and predictable behavior of the ideal model, despite only minor deviations from ideal characteristics. Observe that reducing the transmittance difference between the selected and culled modes from 4% to 2% does not lead to the same mathematically simple result in the fast model [Figs. 8(a) and 8(b)] as in the ideal model [Figs. 2(a) and 2(b)]. Furthermore, note that differences in the initial power distribution can result in striking changes in dynamics in the fast model [Figs. 8(b) and 8(c)], while changes in the ideal model are minimal [Figs. 2(b) and 2(c)].

Consistent with ideal model results when the transmittance of the culled modes is less than the selected mode transmittance, the power tends to concentrate in the selected mode, as shown by Fig. 9. Steady state was not always reached by the end of the simulations. The transition from the selected mode having the majority of the power to the selected mode possessing minimal power occurs suddenly, as the culled mode transmittance exceeds the selected mode transmittance. The curves in Fig. 9 exhibit variability which arises solely from differences in scattering and virtual aperture position.

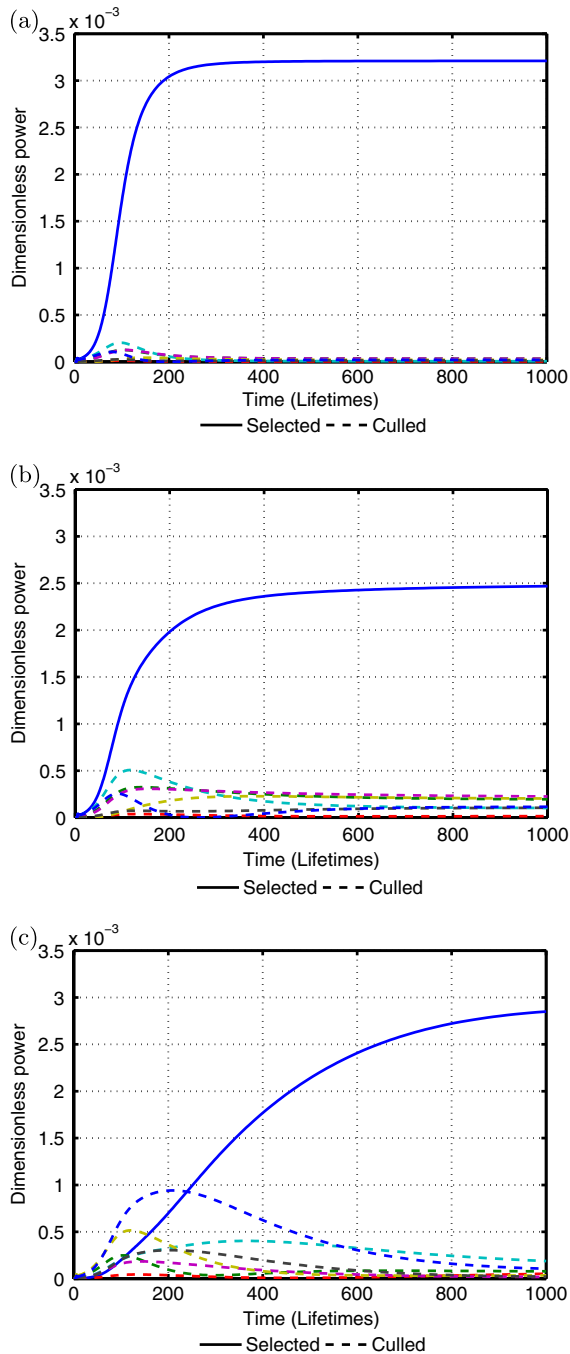


Fig. 8. In these three representative time series of the fast VACER model, virtually all of the circulating power is in the selected mode (solid line) by the end of the simulations, though the power in the seven culled modes (dashed lines) initially rises with the selected mode power. In (a), the transmittance of the culled modes is 4% less than the transmittance of the selected mode, while in (b) and (c), the transmittance of the culled modes is 2% less. Though (a) and (b) result from simulations with the same randomly generated turbid medium, (c) originates from a distinct turbid medium. The turbid media and virtual aperture configurations used in (a)–(c) and in the corresponding plots in Fig. 2 are the same.

The implications of Fig. 9 are clearer for implementation of a virtual aperture with ultrasound than with magnetic fields. Frequency-modulated counterpropagating ultrasonic waves can be generated such that there is only one continual null position. As is the case with magnetic fields, traveling

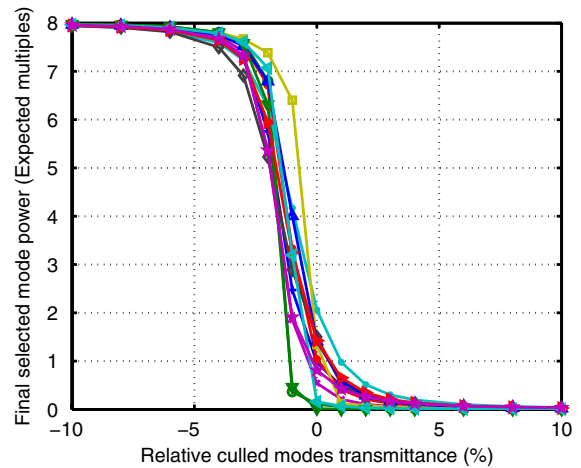


Fig. 9. Final power in the selected mode depends on the transmittance of the culled modes. While most of the power is in the selected mode when culled mode transmittance is less than the selected mode transmittance, the selected mode has little power when culled mode transmittance is greater than the selected mode transmittance. Each plotted curve is from a different randomly generated turbid medium. Furthermore, corresponding curves in this plot and Fig. 6 used the same turbid medium.

ultrasonic waves have an orientation which is not reversed by phase conjugation. The nonreciprocal nature of traveling wave acousto-optic modulation has been exploited for the unidirectional operation of ring lasers [24–27]. If the traveling ultrasonic waves are not time-reversed, then the light lost due to the virtual aperture is approximately the frequency-shifted light. For example, the simulations shown in Figs. 8(b) and 8(c) could represent results when 2% of the light propagating through the volume of the turbid medium inundated by ultrasonic waves is frequency shifted. The effect of magnetic fields is more difficult to estimate because magnetic fields indirectly lead to light loss. Besides magnetic field strength, the polarization of scattering, the distance between scatterers, the orientation of propagation relative to the magnetic field, the magnetic field geometry, and other factors are needed to estimate loss attributable to a magnetic field virtual aperture. Moreover, the light loss due to a magnetic field virtual aperture is a nonlinear function of the aforementioned parameters. For example, light loss has a periodic dependence on distance between scatterers.

5. CONCLUSIONS

With hybrids of widely used models in optics, we have demonstrated that VACER is based on sound physical principles. We have shown the ability of VACER to concentrate light in a single mode within turbid media represented by general linear systems, albeit with only a tiny fraction of the modes possible in media generally considered turbid. Because wave focusing may be interpreted as the consequence of an appropriate superposition of waves, we have demonstrated the feasibility of focusing light at arbitrary positions with VACER. Moreover, the size of the focus could be very small [8,28–31]. Often, little more than the location of the intended target is known, so wavefront shaping is not directly applicable, but in VACER, the location of the intended target is the only needed information. As long as the virtual aperture is centered on the target and there are not any modes circumventing the virtual

aperture, then there is a strong bias for the light to be focused at the target. Even when the mode-filtering mechanism is weak, the concentration of light at the focus can be substantial since the mode filtering mechanism acts on the modes during each pass between the phase conjugate mirrors. Consequently, after many passes, the selected modes generally have significantly more power than the culled modes.

In the computational modeling, whenever the transmittance of the culled modes was greater than the transmittance of the selected modes, power was rarely concentrated in the selected modes as desired. Experimental scenarios are likely to be more forgiving. In any actual virtual aperture implementation, the transmittance will gradually decline from the maximum at the center of the virtual aperture. Thus, even if the virtual aperture is centered at a portion of a turbid medium which happens to attenuate the selected modes enough to prevent their oscillation, the culled modes which do oscillate will almost certainly be near the center of the virtual aperture. Since most of the culled modes will have negligible power and the culled modes which have most of the power will propagate near the center of the virtual aperture, VACER will focus light close to the intended target.

Considering the similarity of the ideal model to previous experimental work with iterative application of TRUE optical focusing [17], implementations of VACER seem inevitable. In particular, experimental implementation of the fast VACER model would enable focusing light within turbid media rapidly enough to escape speckle decorrelation. The parameters used in the fast model are consistent with feasibility. Specifically, the gain, irradiance of the reference beams, and system scale are experimentally feasible. The most significant question about the findings originates from uncertainty about how representative the statistics of the simulated turbid media are to the statistics of real turbid media. Conceiving of scenarios in which VACER would fail to concentrate light is straightforward. Whenever a backscattered or transmitted mode has the lowest loss and bypasses the center of the virtual aperture, an ideal VACER system does not focus light at the target. Nevertheless, the probability of failure in practical cases is difficult to predict, since the loss distribution of modes is the relevant characterization of turbid media rather than the much more familiar bulk scattering properties. In particular, it is unclear how likely a backscattered mode could result in aberrant operation because the backscatter from an individual scatterer is usually weak and multiple scattering tends to distribute light widely leading to significant losses. Nonetheless, the results support the potential for VACER to harmlessly focus light deep within turbid media at arbitrary positions.

ACKNOWLEDGMENTS

This study was supported by the National Institutes of Health (EB011556) and the Coulter Foundation.

REFERENCES

- I. M. Vellekoop and A. P. Mosk, "Focusing coherent light through opaque strongly scattering media," *Opt. Lett.* **32**, 2309–2311 (2007).
- Z. Yaqoob, D. Psaltis, M. S. Feld, and C. Yang, "Optical phase conjugation for turbidity suppression in biological samples," *Nat. Photonics* **2**, 110–115 (2008).
- I. M. Vellekoop, E. G. van Putten, A. Lagendijk, and A. P. Mosk, "Demixing light paths inside disordered metamaterials," *Opt. Express* **16**, 67–80 (2008).
- I. M. Vellekoop and A. P. Mosk, "Universal optimal transmission of light through disordered materials," *Phys. Rev. Lett.* **101**, 120601 (2008).
- M. Cui, E. J. McDowell, and C. Yang, "Observation of polarization-gate based reconstruction quality improvement during the process of turbidity suppression by optical phase conjugation," *Appl. Phys. Lett.* **95**, 123702 (2009).
- M. Cui, E. J. McDowell, and C. Yang, "An in vivo study of turbidity suppression by optical phase conjugation (TSOPC) on rabbit ear," *Opt. Express* **18**, 25–30 (2010).
- M. Cui and C. Yang, "Implementation of a digital optical phase conjugation system and its application to study the robustness of turbidity suppression by phase conjugation," *Opt. Express* **18**, 3444–3455 (2010).
- I. M. Vellekoop, A. Lagendijk, and A. P. Mosk, "Exploiting disorder for perfect focusing," *Nat. Photonics* **4**, 320–322 (2010).
- X. Xu, H. Liu, and L. V. Wang, "Time-reversed ultrasonically encoded optical focusing into scattering media," *Nat. Photonics* **5**, 154–157 (2011).
- Y. M. Wang, B. Judkewitz, C. A. DiMarzio, and C. Yang, "Deep-tissue focal fluorescence imaging with digitally time-reversed ultrasound-encoded light," *Nat. Commun.* **3**, 928 (2012).
- F. Ramaz, B. Forget, M. Atlan, A. C. Boccara, M. Gross, P. Delaye, and G. Roosen, "Photorefractive detection of tagged photons in ultrasound modulated optical tomography of thick biological tissues," *Opt. Express* **12**, 5469–5474 (2004).
- P. Lai, X. Xu, and L. V. Wang, "Ultrasound-modulated optical tomography at new depth," *J. Biomed. Opt.* **17**, 066006 (2012).
- K. Si, R. Fiolka, and M. Cui, "Fluorescence imaging beyond the ballistic regime by ultrasound-pulse-guided digital phase conjugation," *Nat. Photonics* **6**, 657–661 (2012).
- C. Gu and P. Yeh, "Partial phase conjugation, fidelity, and reciprocity," *Opt. Commun.* **107**, 353–357 (1994).
- S. Campbell, P. Yeh, C. Gu, and Q. B. He, "Fidelity of image restoration by partial phase conjugation through multimode fibers," *Opt. Commun.* **114**, 50–56 (1995).
- E. J. McDowell, M. Cui, I. M. Vellekoop, V. Senekerimyan, Z. Yaqoob, and C. Yang, "Turbidity suppression from the ballistic to the diffusive regime in biological tissues using optical phase conjugation," *J. Biomed. Opt.* **15**, 025004 (2010).
- K. Si, R. Fiolka, and M. Cui, "Breaking the spatial resolution barrier via iterative sound-light interaction in deep tissue microscopy," *Sci. Rep.* **2**, 748 (2012).
- W. J. Tom, "Focusing light within turbid media with virtual aperture culling of the eigenmodes of a resonator," Ph.D. dissertation (University of Texas at Austin, 2012).
- S. M. Popoff, G. Lerosey, R. Carminati, M. Fink, A. C. Boccara, and S. Gigan, "Measuring the transmission matrix in optics: an approach to the study and control of light propagation in disordered media," *Phys. Rev. Lett.* **104**, 100601 (2010).
- S. M. Popoff, G. Lerosey, M. Fink, A. C. Boccara, and S. Gigan, "Controlling light through optical disordered media: transmission matrix approach," *New J. Phys.* **13**, 123021 (2011).
- M. Pozniak, K. Zyczkowski, and M. Kus, "Composed ensembles of random unitary matrices," *J. Phys. A* **31**, 1059–1071 (1998).
- L. Shampine and M. Reichelt, "The MATLAB ODE suite," *SIAM J. Sci. Comput.* **18**, 1–22 (1997).
- C. Stockbridge, Y. Lu, J. Moore, S. Hoffman, R. Paxman, K. Toussaint, and T. Bifano, "Focusing through dynamic scattering media," *Opt. Express* **20**, 15086–15092 (2012).
- R. Roy, P. A. Schulz, and A. Walther, "Acousto-optic modulator as an electronically selectable unidirectional device in a ring laser," *Opt. Lett.* **12**, 672–674 (1987).
- M. K. Reed and W. K. Bischel, "Acousto-optic modulators as unidirectional devices in ring lasers," *Opt. Lett.* **17**, 691–693 (1992).

26. W. Clarkson, A. Neilson, and D. Hanna, "Unidirectional operation of ring lasers via the acoustooptic effect," *IEEE J. Quantum Electron.* **32**, 311–325 (1996).
27. Y. Wang, N. Saito, and H. Tashiro, "Unidirectional operation of a ring laser by means of anisotropic acousto-optic device," *Opt. Commun.* **207**, 279–285 (2002).
28. G. Lerosey, J. de Rosny, A. Tourin, and M. Fink, "Focusing beyond the diffraction limit with far-field time reversal," *Science* **315**, 1120–1122 (2007).
29. E. G. van Putten, A. Lagendijk, and A. P. Mosk, "Optimal concentration of light in turbid materials," *J. Opt. Soc. Am. B* **28**, 1200–1203 (2011).
30. E. G. van Putten, D. Akbulut, J. Bertolotti, W. L. Vos, A. Lagendijk, and A. P. Mosk, "Scattering lens resolves sub-100 nm structures with visible light," *Phys. Rev. Lett.* **106**, 193905 (2011).
31. J.-H. Park, C. Park, H. Yu, J. Park, S. Han, J. Shin, S. H. Ko, K. T. Nam, Y.-H. Cho, and Y. Park, "Subwavelength light focusing using random nanoparticles," *Nat. Photonics* **7**, 454–458 (2013).